Stochastic stresses in granular matter simulated by dripping identical ellipses into plane silo

K. N. Berntsen and O. Ditlevsen
Department of Structural Engineering and Materials
Technical University of Denmark, DK-2800 Lyngby. E-mail: knb@bkm.dtu.dk, od@bkm.dtu.dk

ABSTRACT. A two-dimensional silo pressure model-problem is investigated by molecular dynamics simulations. A plane silo container is filled by a granular matter consisting of congruent elliptic particles dropped one by one into the silo. A suitable energy absorbing contact force mechanism is activated during particle collisions and collisions against the walls. After a while the residual kinetic energy is small enough that the granular medium can be considered to be in equilibrium. The sample of contact forces along the wall and the average vertical force components over the horizontal cross-sections through the granular matter in the silo are compared to the solution of a stochastic equilibrium differential equation. In this equation the stochasticity source is a homogeneous white noise gamma-distributed side pressure factor field along the walls. This is a generalization of the deterministic side pressure factor proposed by Janssen in 1895. The stochastic Janssen factor model is shown to be fairly consistent with the observations from which the mean and the intensity of the white noise is estimated by the method of maximum likelihood using the properties of the gamma-distribution. Two wall friction coefficients are determined, one for transforming the expectation and the other for transforming the intensity of the transverse stress factor into the mean and the intensity of the vertical white noise shear stress factor field along the walls. The latter is determined by the observed ratio of the standard deviations of the two fields. The first is estimated by fitting the exponential expectation function for the average normal stress in the horizontal cross-sections to the observed sample function by the principle of least square. Knowing these, in total four, estimated parameter values, the stochastic model determines the expectation function of the stress field normal to the walls, and the covariance functions of all considered stress fields. The observed stress field realizations are not contradicting these predictions. Thus it is demonstrated that molecular dynamics simulations can lead to valuable insight with respect to granular matter behavior even with the limited number of particles that can be handled with practicable computer efforts. Most important is the observation that a gamma-distributed stochastic side pressure field is a valid modeling assumption.

1 INTRODUCTION

[1] The physics of granular matter lack a united continuum mechanics theory. To examine the effects of particle shape, resort is therefore made to slow computational methods such as a molecular dynamics method (a discrete element method) by which the trajectories of the individual particles are followed by integrating Newton's second law numerically in small time steps.

One of the problems that needs to be better understood in silo pressure research is the stochastic nature of the spatial and temporal pressure variation on the silo wall. It has recently been reported in (Holst, Rotter, Ooi, & Rong 1999a, Holst, Rotter, Ooi, & Rong 1999b) that the results from various state-of-the art computational methods — both finite element methods and molecular dynamics methods — applied to this problem yield significantly different results.

This paper reports on computer simulations of silo fillings set up to examine the effect of the particle shape on the silo wall pressures. The purpose is to elucidate some of the sources to the discrepancies in (Holst, Rotter, Ooi, & Rong 1999b), but also to get insight about the stochastic nature of the pressure variations in terms of probability distributions for the wall pressures for different particle shapes.

Moreover a stochastic model for the wall pressure is formulated and solved with respect to mean

[1] to be presented at ICASP'8, Sydney, Dec. 1999. (text corrected Nov. 16, 1999)

and variance of the wall pressure. This stochastic model is a direct extension of the classical Janssen model. The key element of the model is the use of a gamma-distributed white noise field to replace the deterministic side pressure factor introduced by Janssen (Janssen 1895).

The simulation problem for realistically sized systems demands extremely large computer efforts. The presently available computer power dictates that only small two-dimensional systems can be simulated (up to some thousand particles) within a reasonable duration of the simulation of each single realization of the particle system. In spite of this limitation it is believed that the obtained results are useful as sources of insight and inspiration for theory formulation, e. g. (Chang & Gao 1995), and also more directly by pointing at reasonable probability distribution types for application in proposed silo pressure models. This belief is consolidated by the finding that the results of the simulation experiments turn out to be well represented by the proposed stochastic model.

2 SIMULATION OF PARTICLE FILLINGS

2.1 *Model*

The simulated physical system is obtained by filling of a two-dimensional box-shaped silo with up to 2601 identical ellipses with semi major axis a and semi minor axis b ($ab = 1$ unit). The final dimensions of the silo filling is approximately 40 units in width and 200 units in height. The filling method is dripping, that is, the ellipse shaped particles are released from an initial position at the center of the silo and a height a little above the current top particle in the filling. A small initial random velocity and rotation is independently assigned to each particle. When the kinetic energy per particle in the filling is sufficiently small, the next particle is dropped, and so on.

For speeding up the calculation, a relatively large time step has been used to reach the specified kinetic energy level. However, after the chosen number of particles have been deposited, the obtained particle configuration is used to restart the simulation with a smaller time step. [2] The resulting filling configurations are shown in Fig. 1 for the six different ellipse eccentricities $a/b = 1.00$, 1.04, 1.21, 2.25, 3.00, 4.00. It is observed that the configuration for the disks (i.e. $a/b = 1.00$) tend to be crystal like with only very few lines of dislocations. Crystalization is observed also for the close to disk ellipses of eccentricity 1.04, but the dislocation lines are much more dense then for the disks. A polymorph configuration structure is observed for the remaining larger eccentricities.

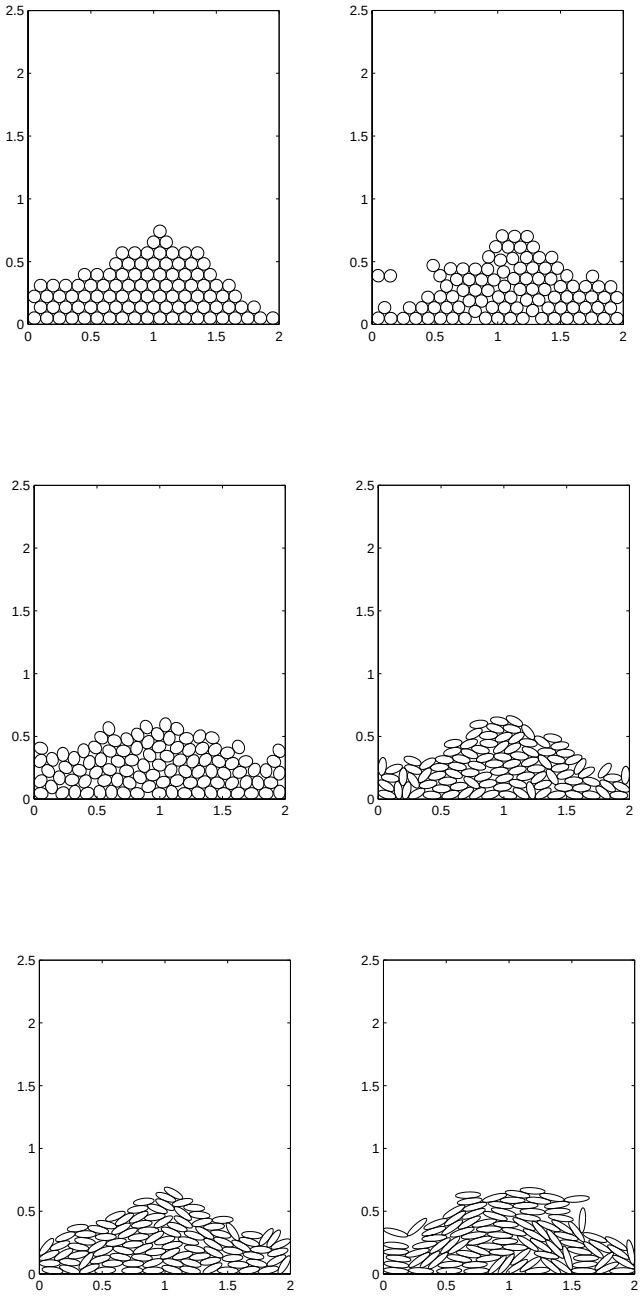

Figure 1. Silo fill configurations for the first dropped 400 elliptic particles of eccentricities 1.00, 1.04, 1.21, 2.25, 3.00, 4.00, respectively. The geometric dimensions are non-dimensionalized by dividing by half the silo width R.

The overlap detection of ellipses is crucial for a molecular dynamics algorithm (see (Allen & Tildesley 1987) for an introduction to MD simulations). Some early contact detection algorithms are criticized in (Ting 1992) and a suggested new algorithm is shown by examples to be suited for

[2] By an unfortunate flaw in the planning of the extremely time demanding simulations the velocities $\dot{\varepsilon}$ (see eq 1) were not registered in the data files after completion of the filling. Therefore the system is restarted a little further away from the equilibrium state as when the filling was completed. This defect of the simulation seems not to effect the physics significantly

handling cases that the earlier algorithms could not handle. The algorithm used for the simulations reported herein is published in (Perram, Rasmussen, Praestgaard, & Lebowitz 1996). This algorithm can also handle all the special cases considered in (Ting 1992). The algorithm allows for an easy overlap estimation of the linear overlap ε along the line connecting the two centers of mass. For small overlaps this linear measure is sufficiently accurate. Needless to say that the simulations with disks are run with a much simpler and faster algorithm for detecting overlaps.

The linear spring dash-pot model is used for the contact forces normal to the particle or wall surfaces. It reads

$$F_n = k\varepsilon + \nu\dot{\varepsilon}, \tag{1}$$

where k is a spring constant and ν is a damping constant. The linear spring dash-pot model and other applicable contact force models are discussed in (Schäfer, Dippel, & Wolf 1996, Luding 1998).

To model the shear contact force between two particles or between a particle and the wall a tangential non-linear elastic spring is attached during contact such as proposed by (Cundall & Strack 1979). For the simulations reported herein the following algorithm is used. It is

$$F_\mu(t) = \begin{cases} \min\{\mu F_n(t), F_e(t)\} & \text{for } F_e(t) \geq 0 \\ \max\{-\mu F_n(t), F_e(t)\} & \text{for } F_e(t) < 0 \end{cases} \tag{2}$$

$$F_e(t) = -\alpha k \int_0^t v_r(\tau)\, d\tau \tag{3}$$

where k is the spring constant in (1), α is a scaling factor ($\alpha = 2/7$ in the present simulations) and v_r is the relative tangential velocity at the contact point between the two particles during contact. This mechanism does not provide tangential damping between the particles. For the wall contacts a tangential viscous damping element is added.

The specific rules (1) to (3) can be criticised for not providing damping of Coulomb dry friction type. In simulations to be made later, a dry friction rule will be built in. An important goal is to investigate to which extend the particle contact force rules have influence on the macroscopic stochastic behavior of the granular matter. Clearly an investigation of which macroscopic properties are insensitive to various contact force rules is of essential physical and technical interest.

2.2 *Parameters in the simulations*

The physical units are chosen such that the ellipses have the mass $m = 0.01$kg and the geometric dimension $ab = 1\text{cm}^2$. The force constants are chosen as $k = 1.8\ 10^5\text{kg s}^{-2}$, $\nu = 40\text{kg s}^{-1}$ and the friction coefficient as $\mu = 0.9$. The gravitational pull is $g = 9.82\ \text{ms}^{-2}$. Letting the known expression $t_c = \sqrt{m/k}$ for the contact time for colliding disks with a pure Hookean interaction as an estimate be the same for the contact time for the ellipses, the contact time becomes $t_c \sim 10^{-3}$ s. The integration is made by a simple Euler scheme with a time step of 10^{-5} s (10^{-4} s initially in the initial phase).

The ellipse eccentricities $e = a/b$, the corresponding number of particles, and the width of the silo used in the simulations is reproduced in Table 1.

Table 1. Number N of particles and width $2R$ of silo for the eccentricity e:

e:	1.0	1.04	1.21	2.25	3	4
N:	2601	2067	2495	2115	1889	1598
$2R$:	40	40.80	39.6	42.0	41.57	40

3 THEORY

3.1 Gamma-distribution

The density of the gamma-distribution with parameters k and λ is

$$f(x;k,\lambda) = \frac{(\lambda x)^{k-1}\lambda e^{-\lambda x}}{\Gamma(k)}, \quad x \geq 0 \tag{4}$$

where $\Gamma(\cdot)$ is the gamma function. The mean is k/λ and the variance is k/λ^2, i.e. the coefficient of variation is independent of λ and equal to $k^{-1/2}$. The gamma-distributed family of independent random variables corresponding to the same value of λ has the property of being closed with respect to addition. If such random variables X_1 and X_2 have parameter values (k_1, λ) and (k_2, λ), respectively, then $X_1 + X_2$ has the parameter values $(k_1 + k_2, \lambda)$.

In (Mueth, Jaeger, & Nagel 1998) it is found experimentally for spheres in small cylinders that the wall contact forces are approximately exponentially distributed corresponding to the case $k = 1$ in the gamma-distribution family. In (Radjai, Jean, Moreau, & Roux 1996) the particle-particle forces obtained in contact dynamics simulations are investigated. It is found that after division of the forces by the average of the forces, a power law distribution with an exponential tail is obtained; the power law is adopted below the mean 1 and the exponential tail is adopted above the mean and the two parts are joined together continuously at the mean. In (Berntsen & Ditlevsen 1999) particle-particle forces obtained in simulations with ellipses and disks are found to fit well with gamma-distributions. Silo wall pressures in a real concrete silo for barley grains have also been observed to fit well with gamma-distributions (Ditlevsen & Berntsen 1999).

3.2 Stochastic Janssen model

For a vertically placed cylindric silo, the classical Janssen assumption is that there between the macroscopic homogeneous silo medium and the silo wall at the position ξ below the horizontal surface ($\xi = 0$) of the medium is a normal stress $K\sigma(\xi)$, where K is a constant and $\sigma(\xi)$ is the vertical stress assumed to be constant over the considered horizontal cross-section through the medium, (Janssen 1895). Moreover, Janssen assumed that there is a constant coefficient of friction μ between the medium and the wall. Then the requirement of static equilibrium directly gives the differential equation (for a two-dimensional silo) $R\,d\sigma(\xi)/d\xi + \mu K\sigma(\xi) = \gamma R$, where R is half the width of the silo medium and γ is the gravity weight density of the medium. Introducing the dimensionless variables $x = \xi/R$, $S(x) = \sigma(\xi)/R\gamma$, $G = K\mu$, the equilibrium equation reduces to

$$\frac{dS}{dx} + GS = 1 \tag{5}$$

With G being a constant the solution that satisfies the boundary condition $S(0) = 0$ is $S(x) = [1 - \exp(-Gx)]/G$. Asymptotically as $x \to \infty$ the dimensionless stress $S(x)$ approaches the constant value $1/G$ and the dimensionless wall stress approaches the value $K/G = \mu^{-1}$, that is, a value independent of the factor K. These results are classical. However, no randomness is contained in this model unless a stochasticity source is introduced in the equilibrium equation (5). The only place for this is to change the constant G to be a random function (random field) $G(x)$. Thus (5) becomes a parametric excited stochastic differential equation. The explicit solution to (5) is

$$S(x) = \int_0^x \exp\Big[-\int_u^x G(t)\,dt\Big]du \tag{6}$$

Inspired by the empirical findings, we will make the simple assumption that $G(x)$ is gamma-distributed white noise of constant mean $E[G(x)] = \kappa$ and covariance function $\mathrm{Cov}[G(x_1), G(x_2)] = I\delta(x_2 - x_1)$, where $\delta(\cdot)$ is Dirac's delta function and I is the intensity of the white noise. The implication is that integrals of the form $\int_u^x G(t)\,dt$ become gamma-distributed with parameters $k = (x-u)\kappa^2/I$ and $\lambda = \kappa/I$, and that any two integrals over disjoint intervals become stochastically independent.

Easy standard arguments give

$$E\Big[\exp\Big(-\int_u^x G(t)\,dt\Big)\Big] = \Big(\frac{\lambda}{\lambda+1}\Big)^{\lambda\kappa(x-u)} \tag{7}$$

$$\mathrm{Cov}\Big[\exp\Big(-\int_{u_1}^x G(t)\,dt\Big), \exp\Big(-\int_{u_2}^{x+\Delta x} G(t)\,dt\Big)\Big]$$

$$= \mathrm{Var}\Big[\exp\Big(-\int_{\max\{u_1,u_2\}}^x G(t)\,dt\Big)\Big]\cdot$$

$$E\Big[\exp\Big(-\int_{\min\{u_1,u_2\}}^{\max\{u_1,u_2\}} G(t)\,dt\Big)\Big]E\Big[\exp\Big(-\int_x^{x+\Delta x} G(t)\,dt\Big)\Big] \tag{8}$$

where $u_1, u_2 \le x$ and $\Delta x \ge 0$. The variance term in (8) is

$$E\Big[\exp\Big(-2\int_{\max\{u_1,u_2\}}^x G(t)\,dt\Big)\Big] - E\Big[\exp\Big(-\int_{\max\{u_1,u_2\}}^x G(t)\,dt\Big)\Big]^2 \tag{9}$$

The factor 2 on the first integral has the simple effect that the parameter λ of the gamma-distribution changes to $\lambda/2$ while $k = \lambda\kappa(x-u)$ remains unchanged. Thus (7) can be directly used to obtain the mean value $[\lambda/(\lambda+2)]^{\lambda\kappa(x-u)}$. Hereafter integrations lead to the results

$$E[S(x)] = \frac{1}{\lambda\kappa\log(1+\lambda^{-1})}\Big[1 - \Big(\frac{\lambda}{\lambda+1}\Big)^{\lambda\kappa x}\Big] \tag{10}$$

$$\mathrm{Var}[S(x)] = \frac{2}{(\lambda\kappa)^2\log\dfrac{\lambda}{\lambda+1}}\left(\frac{1-\Big(\dfrac{\lambda}{\lambda+2}\Big)^{\lambda\kappa x}}{\log\dfrac{\lambda}{\lambda+2}}\right.$$

$$\left. - \frac{1-\Big(\dfrac{\lambda+1}{\lambda+2}\Big)^{\lambda\kappa x}}{\log\dfrac{\lambda+1}{\lambda+2}}\Big(\frac{\lambda}{\lambda+1}\Big)^{\lambda\kappa x} - \frac{\Big[1-\Big(\dfrac{\lambda}{\lambda+1}\Big)^{\lambda\kappa x}\Big]^2}{2\log\dfrac{\lambda}{\lambda+1}}\right) \tag{11}$$

$$\frac{\mathrm{Cov}[S(x), S(x+\Delta x)]}{\mathrm{Var}[S(x)]} = \Big(\frac{\lambda}{\lambda+1}\Big)^{\lambda\kappa|\Delta x|} \tag{12}$$

$$\frac{\mathrm{Var}[S(\infty)]}{E[S(\infty)]^2} = \frac{\log[(1+\lambda^{-1})^2/(1+2\lambda^{-1})]}{\log(1+2\lambda^{-1})} \propto \frac{1}{2\lambda} \tag{13}$$

asymptotically as λ increases. The conclusion is that the normal stress $S(x)$ approaches a statistically homogeneous state as $x \to \infty$ such as it is also seen in the simulation experiments.

It follows from the differential equation (5) and from (10) that

$$E[G(x)S(x)] = 1 - \frac{dE[S(x)]}{dx} = 1 - \Big(\frac{\lambda}{\lambda+1}\Big)^{\lambda\kappa x} \tag{14}$$

which approaches 1 as $x \to \infty$.

Obviously the variance of $G(x)S(x)$ is infinite, but physically what is observed is an average over some small height h. For small h this averaging does not change the mean by much, but it has a

large effect on the variance. Actually, from the differential equation it follows that

$$E\Big[\frac{1}{h}\int_0^h G(x+t)S(x+t)\,dt\Big]$$

$$=1-\frac{1}{h}\Big(E[S(x+h)]-E[S(x)]\Big)\to 1 \qquad (15)$$

$$\mathrm{Var}\Big[\frac{1}{h}\int_0^h G(x+t)S(x+t)\,dt\Big]=\frac{1}{h^2}\mathrm{Var}[S(x+h)-S(x)]$$

$$\to \frac{2}{h^2}\Big(1+\frac{\lambda}{1+\lambda}\Big)^{\lambda\kappa h}\mathrm{Var}[S(\infty)] \qquad (16)$$

as $x\to\infty$. The factor on the right side varies asymptotically like $2\lambda\kappa\log(1+\lambda^{-1})/h$ as $h\to 0$. For finite x the variance on the left side of (16) is calculated by use of (11) and (12).

In the following analysis of the data obtained from the silo filling simulations, this stochastic Janssen model is compared to the simulated empirical data. In this paper no attempt is made to investigate the joint stochastic properties of the wall shear stress factor field $G(x)=\mu(x)K(x)$ and the transverse stress factor field $K(x)$. As a simplification it is assumed that the influence of the wall friction coefficient $\mu(x)$ can be modeled accurately enough by use of two constants μ_m and μ_I such that $\kappa=\mu_m E[K]$ and $I=\mu_I^2 I_K$, where I_K is the intensity of the field $K(x)$, assumed like $G(x)$ to be homogeneous gamma-distributed white noise. When $G(x)$ is replaced by $K(x)$ in (15) and (16) the right-hand sides must be divided by μ_m and μ_I^2, respectively.

4 COMPARISON OF STOCHASTIC MODEL WITH SIMULATION RESULTS

To non-dimensionalize the stresses, the weight density γ has been calculated from the fillings. There is a minor dependence on the eccentricity, but in the present context it is sufficiently accurate to put the void ratio to 0.8.

The directly observed wall force per length unit (= particle size ab) has strongly scattering variation along the walls. This appearance makes it a tractable idea to apply white noise modeling as suggested in the previous section. Guided by the model considerations of the previous section the ratio $K(x)=S_w(x)/S(x)$ of the observed dimensionless wall stresses $S_w(x)$ orthogonal to the wall (in fact, the average of the stresses at the two opposite wall points at x) and the observed dimensionless vertical average stress $S(x)$ over the cross-section of the silo at level x has been calculated. For four examples of ellipse eccentricities the observed vertical stresses $S(x)$ are plotted as function of x in Figs. 3 to 7. The same figures show the moving averages over a window size $h=0.5$ of $S_w(x)$, and moreover Figs. 4 to 7 show the moving averages of $K(x)$ and $\mu(x)$. It is seen that the stresses tend to statistical homogeneity for increasing x. Even more interestingly, for the four largest eccentricities the ratio $K(x)$ has a statistically homogeneous (most visible for $e=1.21$ and $e=2.25$) and white noise like appearance over the entire height except possibly for a small interval at the top of the filling. This observation is qualitatively consistent with the formulated stochastic model.

An increase of $S(x)$ over a short distance near the bottom of the silo is common to all fillings. This is an effect of the bottom boundary condition. Obviously the wall shear stress must vanish at the bottom. The equilibrium condition then dictates that the vertical stress near the bottom must increase beyond the stress observed if the bottom is in infinite depth.

For the disk fillings ($e=1$) the vertical stress variation with x is almost hydrostatic in the upper quarter of the filling implying that the stress factor $K(x)$ along the upper quarter of the walls is almost vanishing in this domain. This behavior of $K(x)$ may be related to the strong crystalization tendency for the disk system, but it may also be due to remaining larger than average amount of kinetic energy per particle in the top of the silo. This higher granular temperature makes the matter act like a hydrostatic liquid. The stochastic model may be applicable in the lower three quarter end of the silo by imposing a boundary stress condition at the the lower level of the top hydrostatic layer. This possibility is not investigated in the present paper. Also the fillings with ellipses close to disks ($e=1.04$) to some extend shows a behavior that deviates from the typical behavior of the fillings with ellipses of larger eccentricities. In both cases the assumption of homogeneity of $K(x)$ along the walls is not well satisfied. This is clearly revealed when attempting to estimate the intensity of the equivalent white noise as explained in the following. Consequently focus will be on the four larger eccentricity cases with small tendency to crystalization.

To justify the model assumption that $K(x)$ is gamma-distributed white noise, the cumulative empirical distribution functions are calculated for the moving average data for a variety of window sizes h, and the parameters $k=k(h)$ and $\lambda=\lambda(h)$ in the gamma-distribution (4) are estimated by the method of maximum likelihood. If $K(x)$ is homogeneous white noise, the relations $\kappa_K=k(h)/\lambda(h)$ and $I_K=hk(h)/\lambda(h)^2$ hold, that is, these func-

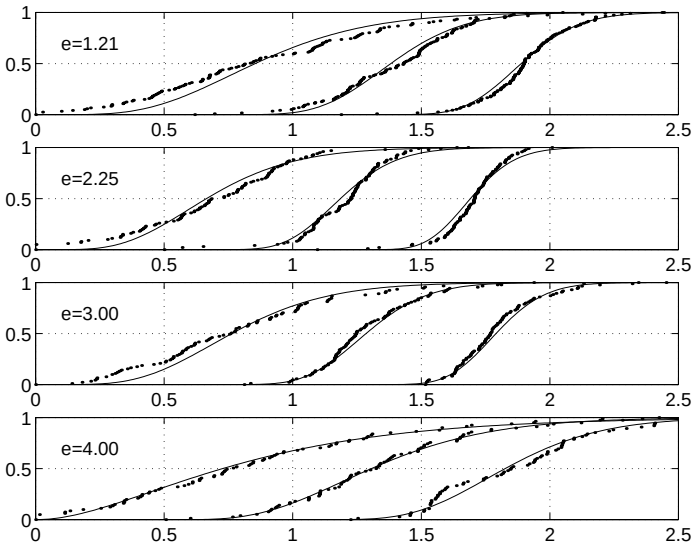

Figure 2. Empirical distribution functions of the moving average data of the side pressure factor $K(x)$ for window sizes $h = 0.2, 0.5, 0.8$ (left to right) compared to gamma-distribution functions that have parameters corresponding to fixed mean κ_K and intensity I_K of the assumed gamma-distributed white noise field $K(x)$ as given in Table 2. The two distribution functions for $h = 0.5, 0.8$ are shifted to the right by 0.5 and 1.0, respectively.

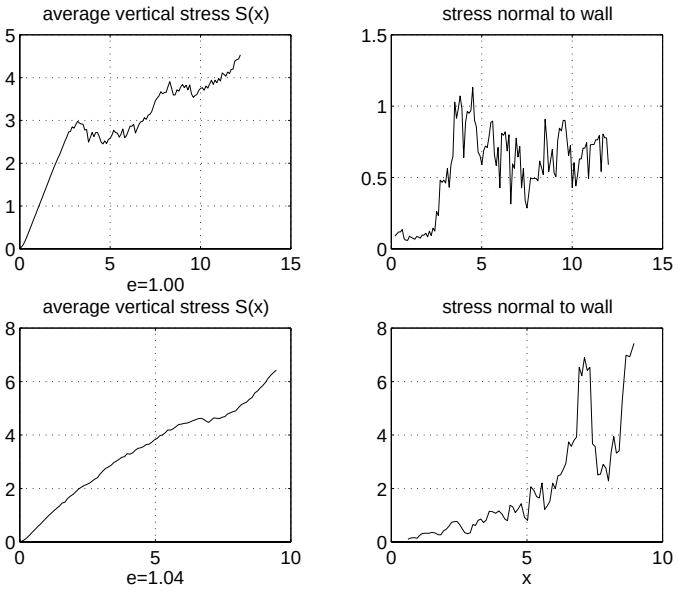

Figure 3. Sample curves for the vertical average stress component $S(x)$ over a horizontal cross-section of the silo and the moving average stress $K(x)S(x)$ normal to the wall defined as the average between the stresses at the points in level x on the two opposite walls of the silo, where x is measured from the top surface position of the granular matter. The averaging window has size $h = 0.5$.

tions of h are the constants $E[K] = \kappa_K$ and I_K (intensity of the white noise). For the real data this should not be expected to hold for small h due to possible auto-correlation on a small scale. In fact, for sufficiently small h there are zeros in the otherwise positive observation series, of course. These zeros create negative auto-correlation. Clearly the stress concept, to have reasonable physical meaning, requires a not too small window size. On

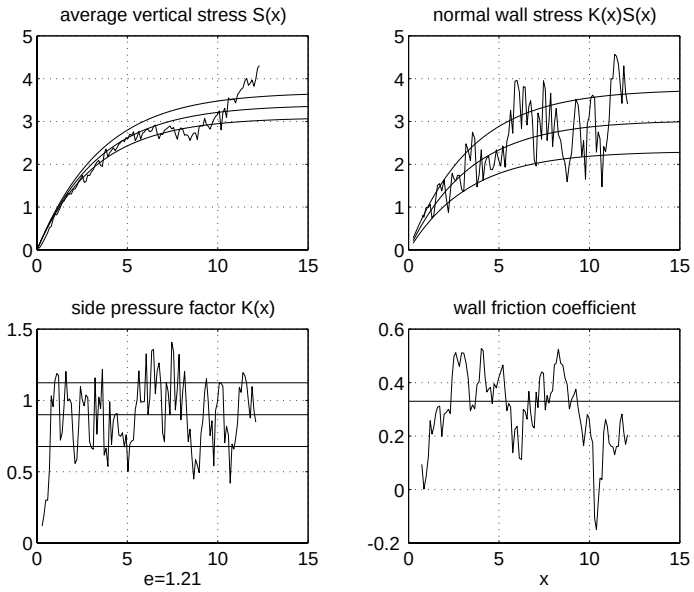

Figure 4. Text as in Fig. 3 for the two top diagrams. The bottom diagrams show the moving average sample functions of the side pressure field $K(x)$ to the left and of the friction coefficient $\mu(x)$ to the right as the average from the two walls of the silo for the window size $h = 0.5$. The three curves in each of the three of the four diagrams come from fitting four parameters of the theoretical model to the data as the mean value function and the mean value function $\pm$ the standard deviation function.

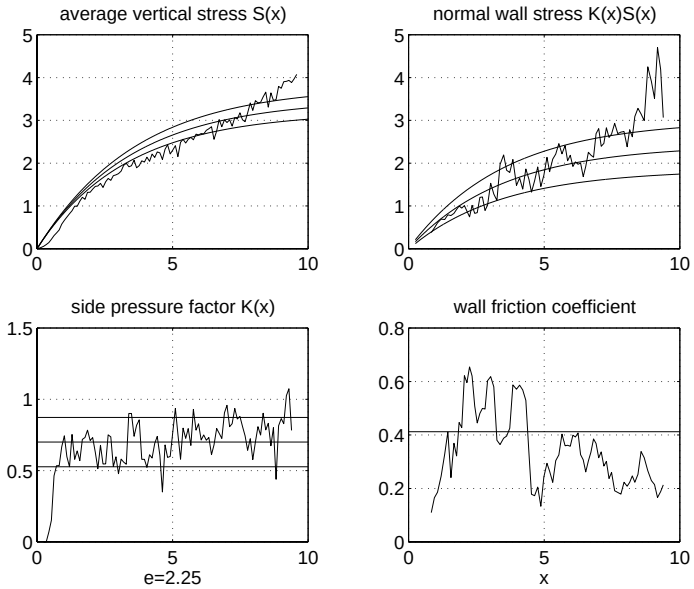

Figure 5. Text as in Fig. 4.

the other hand, when the window size is taken so large that the number of independent averages becomes small, the effect of statistical uncertainty becomes dominating. What should be expected then is that the above functions have a tendency to reach a constant level in some intermediate range of window sizes. For the data corresponding to the four largest eccentricities this level tendency is observed in a range of h from about 0.3 to about 0.7. Fig. 2 shows the empirical distribution functions in the four eccentricity cases for the three window sizes $h = 0.2, 0.5, 0.8$ together with the gamma-

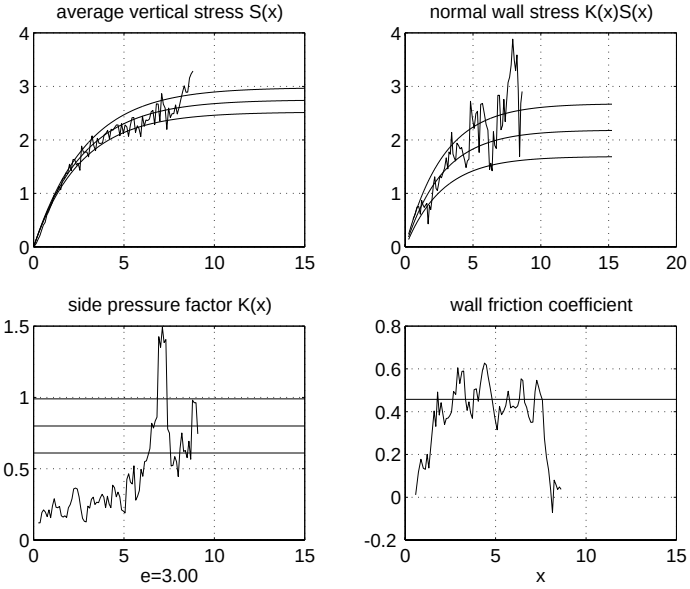

Figure 6. Text as in Fig. 4.

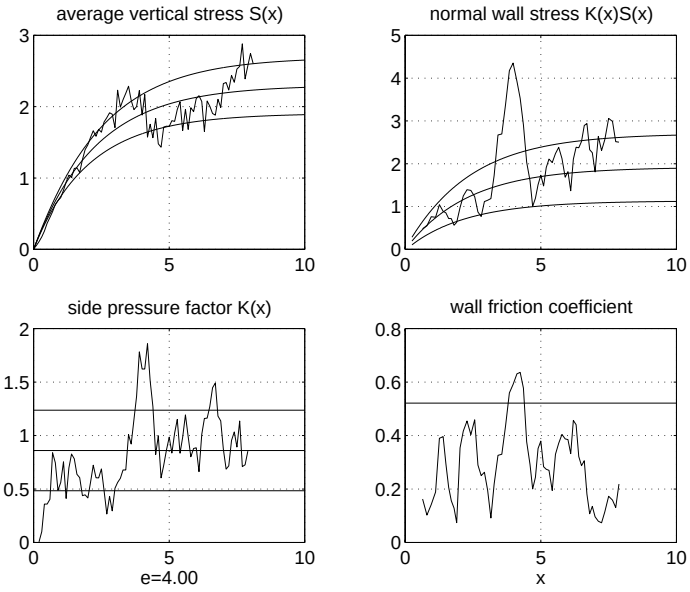

Figure 7. Text as in Fig. 4.

distribution functions corresponding to the parameter values given in Table 2. These values are judgmentally estimated from considering the aforementioned levels of approximate constancy. It is seen from Fig: 2 (in which the distribution functions for $h = 0.5$ and $h = 0.8$ for the sake of separating the data are shifted to the right by 0.5 and 1.0, respectively) that the model fits reasonably well in the considered range of h (as expected less well, though, for $h = 0.2$ than for the two larger values of h).

Table 2. Estimates of mean $\kappa_K = \kappa/\mu_m$ and intensity $I_K = I/\mu_I^2$ of the side pressure factor $K(x)$ corresponding to the eccentricity e:

e :	1.21	2.25	3.00	4.00
κ_K :	0.90	0.70	0.80	0.86
I_K :	0.25	0.15	0.18	0.71

After gaining this interesting experience the next step is to obtain estimates of the "equivalent" friction coefficients μ_m and μ_I. The model predicts the exponential expectation function (10) for the stress $S(x)$. Thus the asymptotic level $\alpha = [\lambda\kappa\log(1+\lambda^{-1})]^{-1}$ may be estimated by a least square fit of the exponential function $\alpha[1 - \exp(-x/\alpha)]$ to the sample function of $S(x)$ (which due to the averaging over the entire horizontal cross-sections are much less fluctuating than the wall stresses). Since $\lambda = \kappa_K\mu_m/I_K\mu_I^2$ and $\kappa = \kappa_K\mu_m$, the value of μ_m can be calculated for each given value of μ_I. This last value is estimated as the ratio of the empirical standard deviations obtained from the observations of the shear force factor field $\mu(x)K(x)$ and the side pressure factor field $K(x)$. The results of this estimation procedure are given in Table3.

Table 3. Estimates of equivalent wall friction coefficients μ_m and μ_I corresponding to the eccentricity e:

e :	1.21	2.25	3.00	4.00
μ_m :	0.330	0.412	0.458	0.521
μ_I :	0.425	0.528	0.534	0.625

Hereafter all relevant mean value functions and standard deviation functions (the last except for the field $\mu(x)$) in the model are uniquely defined. The results are plotted in Figs. 4 to 7, and they are seen to behave quite reasonably except that they do not take the bottom boundary condition into account, of course. The estimated values of μ_m are also shown together with the moving average observations of $\mu(x)$. Except for the case $e = 4.00$, the estimated equivalent friction coefficients are not on the average deviating with substantial bias from the observed values of $\mu(x)$.

The results should be judged having in mind that all the empirical curves are from a single realization of the filling for each considered ellipse eccentricity. The consumption of computer time to make each filling is very large. This presently sets a limit to the number of repetitions it is realistic to generate. Such repetitions will give other fluctuations that most likely will show convincingly that the specific fluctuations seen in the figures are of pure random nature. On the other hand, these isolated simulations make it difficult to come up with firm conclusions on the dependency of the parameters on the ellipse eccentricity.

5 CONCLUSIONS AND FURTHER INVESTIGATIONS

It is shown by a two-dimensional model problem that molecular dynamics simulations with a rather limited number of particles in play can reveal realistic continuum mechanics features of a granular matter filled into a silo. Fillings with congruent

ellipses show the expected saturation behavior as described in the classical theory of Janssen. Most interestingly the granular matter simulations reveal a side pressure factor (the ratio of normal wall stress to vertical stress in the granular matter) that approximately behaves like a homogeneous gamma-distributed white noise field. On the basis of this experience a stochastic equilibrium equation of Janssen type is formulated. Using the assumption that the vertical shear stress factor is gamma-distributed white noise, it is possible by elementary mathematical calculations to solve this parametric excited differential equation with respect to mean value functions and covariance functions. Moreover, by estimating only four parameters (mean and intensity of side pressure factor and moreover two "equivalent" wall friction coefficients) from the observed data it is further possible to uniquely calculate all the relevant solution functions of the model. The comparison with the observed sample functions are reasonably convincing about the applicability of the model.

Some further simulation investigations and theoretical analyses might be on the following points:

1. Make some more simulated fillings without change of the controlled parameters.

2. Investigate the influence of the silo width on the parameters of the model and the limitations of the generalized Janssen model.

3. Consider the influence of using different reasonable particle contact force rules including Coulomb dry friction rules that give substantial hysteresis damping.

4. Analyze the data of all contact forces within the body of the granular matter in the silo with respect to the stochastic properties of a local side pressure factor field of Janssen type.

5. Make simulations of open heaps of granular matter of ellipses to investigate the same question as raised in point 4.

ACKNOWLEDGEMENTS

This work has been financially supported by the Danish Technical Research Council.

REFERENCES

Allen, M. P. & D. J. Tildesley (1987). *Computer Simulation of Liquids*. Oxford: Oxford University Press.

Berntsen, K. N. & O. Ditlevsen (1999). Granular systems of ellipses, packing and orientational ordering. Unpublished.

Chang, C. S. & J. Gao (1995). Second-gradient constitutive theory for granular material with random packing structure*Int. J. Solids and Structures* 32(16):2279–2293.

Cundall, P. A. & O. D. L. Strack (1979). A discrete numerical model for granular assemblies*Géotechnique* 29(1):47–65.

Ditlevsen, O. & K. N. Berntsen (1999, May). Empirically based gamma-distributed stochastic wall pressure field in silo*Journal of Engineering Mechanics, ASCE* 125(5):561–569.

Holst, J. M. F. G., J. M. Rotter, J. Y. Ooi, & G. H. Rong (1999a). Numerical modeling of silo filling. in: Continuum analysis *Journal of Engineering Mechanics, ASCE* 125(1):94–103.

Holst, J. M. F. G., J. M. Rotter, J. Y. Ooi, & G. H. Rong (1999b). Numerical modeling of silo filling. ii: Discrete element analysis*Journal of Engineering Mechanics, ASCE* 125(1):104–110.

Janssen, H. A. (1895). Versuche über getreidedruck in silozellen*Zeitschrift des Vereins Deutcher Ingenieure* 39(35):1045–1049.

Luding, S. (1998). Collisions & contacts between two particles. In H. J. Herrmann, J.-P. Hovi, & S. Luding (eds.), *Physics of dry granular media - NATO ASI Series*, Dordrecht, pp. 285. Kluwer Academic Publishers.

Mueth, D. M., H. Jaeger, & S. R. Nagel (1998). Force distribution in a granular medium*Physical Review E* 57(3):3164–3169.

Perram, J. W., J. Rasmussen, E. Praestgaard, & J. L. Lebowitz (1996). Ellipsoid contact potential: Theory and relation to overlap potentials*Phys. Rev. E.* 54(5):6565–6572.

Radjai, F., M. Jean, J. J. Moreau, & S. Roux (1996). Force distribution in dense two-dimensional granular systems*Phys. Rev. Lett.* 77(2):274.

Schäfer, J., S. Dippel, & D. Wolf (1996). Force schemes in simulations of granular materials. *J.Phys. I France* 6:5–20.

Ting, J. M. (1992). A robust algorithm for ellipse-based discrete discrete element modelling of granular materials. *Comput. Geotech* 13:175–186.